Diagnosis of a Unit-Wide Disturbance Caused by Saturation in a Manipulated Variable

Toru Matsuo+, Isao Tadakuma+ and Nina F. Thornhill*
+Mitsui Chemicals, Omuta Works, Japan
** Department of Electronic and Electrical Engineering, University College London*
E-mail: n.thornhill@ee.ucl.ac.uk

Abstract

It is well known that faulty control valves with friction in the moving parts lead to limit cycle oscillations which can propagate to other parts of the plant. However, a control loop with a healthy valve can also undergo oscillatory behavior. The root cause of a unit-wide oscillation in a distillation column was traced to a pressure control loop in a case study at Mitsui Chemicals. The diagnosis was made by means of a new technique of pattern matching of the time-resolved frequency spectrum using a wavelet analysis tool. The method identified key characteristics shared by measurements at various places in the column and quantified the similarities.

Non-linearity was detected in the time trend of the pressure measurement, a result which initially suggested the root cause was a faulty actuator or sensor. Further analysis showed, however, that the source of non-linearity was periodic saturation of the manipulated variable caused by slack tuning. The problem was remedied by changing the controller tuning settings and the unit-wide disturbance then went away.

1. Introduction

Computerized DCS (distributed control systems) and the use of digital data for controlling the process have been prevalent since the 1980s in chemical plants. More recently, data historians which store information about the long-term operational behavior of plant have led to applications involving the analysis and extraction of information from the stored data.

The ability to collect, observe and analyze historical data trends has led to concerns about the effects of process variability on the economics of a process [1]. The situation is made worse if an oscillatory disturbance originating in one part of the plant becomes widespread due to physical coupling and recycles. It can propagate from its source causing numerous secondary oscillations. A key issue is to determine the root cause of such a plant-wide oscillation [2] and calls are growing from industrial manufacturers for the automated detection and diagnosis of plant-wide oscillations [3].

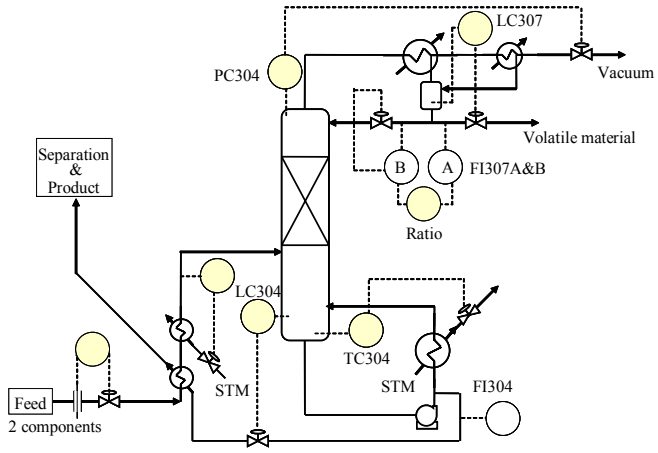

Figure 1. Distillation column with a unit-wide oscillation

This article contributes to the detection and diagnosis of a widespread oscillation through the application of wavelet analysis. *Time2Wave* is a new frequency analysis tool created by Yamatake Corporation and co-developed with Mitsui Chemicals for the purposes of analyzing historical process data from chemical plants. It has a plant-wide focus with the ability to align the wavelet patterns from multiple tags and to determine a measure of the similarity between them. The article presents these tools and explores their capability.

A major cause of plant-wide oscillation is sticking valves that cause a limit cycle under feedback. Several solutions have now been proposed for the detection and diagnosis of sticking valves [4-6]. However, the case study at Mitsui Chemicals reported here has shown that even a healthy valve can cause a limit cycle oscillation and there is thus a need to revisit the diagnosis step to ensure that the correct diagnosis is achieved. A diagnostic signature derived from the plant measurements that is sensitive to manipulated variable saturation is proposed to

augment previous work in automated root cause diagnosis.

All methods are illustrated with data from an industrial distillation column courtesy of the Omuta works of Mitsui Chemicals. The process schematic is in Figure 1 and the measurements from the plant are shown in Figure 2.

2. Background

The most basic application of a data historian is the plotting of time trend data, with advanced tools being available for subsequent observation and diagnosis by skilled engineers who use them to extract characteristics from the trend graph [7].

Frequency-domain analysis is of value when measured time domain signals have oscillatory behavior. Newton demonstrated the presence of various frequencies (color of light) being contained in the light by utilizing prism refraction. It may be regarded as the first demonstration of a signal transform into the frequency domain. In chemical plants, the condition of rotating machinery is monitored using a vibration meter combined with a spectral analysis. In this area, for instance, [8] reviewed advanced on-line spectral condition-monitoring sensors for use with the reactor coolant pump in nuclear power station while [9] focused on fault detection and preventive maintenance of process machinery.

Frequency analysis may be applied to any measured time trend including those from chemical processes which vary with long periods of many minutes or even hours. The discrete Fourier transform (DFT) is the fundamental algorithm applied and the power spectrum is the normalized squares of the magnitudes of the DFT. In the case of a persistent oscillation in the time trend the power spectrum gives a clear signature for the oscillation since is has a sharp peak (large magnitude) at the frequency of the oscillation.

However, it is not always the case that oscillatory features are persistent. Figure 2 shows exampled of process data in which short bursts of oscillatory behavior may be seen, for instance in tags 6 to 9 starting just after sample 3000. The technique of the Wavelet transform and algorithms for its computation [10,11] enabled frequencies to be analyzed in a time-resolved mode, allowing the approaches to frequency analysis to be widened further [12, 13]. The algorithm allows the time-dependent variable characters of the frequency to be extracted from the time-series data. The wavelet transform provides a signal amplitude as a function of frequency of oscillation (the resolution) and time of occurrence. One method of presentation shows times and resolution plotted on the horizontal and vertical axes and amplitudes represented by hues in the contour lines corresponding to them on the time-frequency plane.

Wavelet analysis of process data has been successfully applied in the past for classification of experimental data for process fault diagnosis[14], multi-scale modeling [15] and its applications in machinery condition monitoring have been recently reviewed by Peng and Chu [16]. Misra et al [17] used wavelets combined with PCA to extract correlation at each scale for the purposes of multivariate fault detection. An earlier study showed that wavelet analysis can successfully address the problem of plant-wide disturbance analysis [18].

3. Methods

3.1. Wavelet transform

A wavelet transform matches the time localization to the frequency of interest using fine time resolution for higher frequencies and coarse time localization for low frequencies.

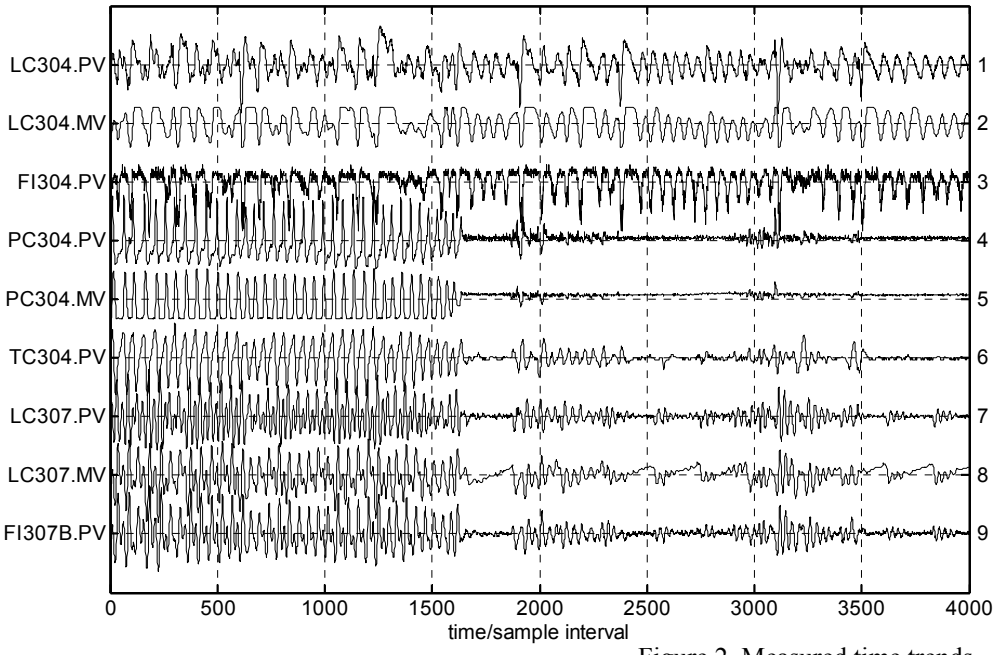

Figure 2. Measured time trends

A wavelet decomposition has the following form:

$$f(x) = a_o\phi(x) + a_1 W(x) + a_2 W(2x) + a_3 W(2x-1) + \ldots + a_{2^j+k} W(2^j x - k) + \ldots$$

where $k = 0$ to $2^j - 1$ and the index i for the wavelet coefficients a_i ranges from 0 to $N-1$, where N is the number of measurements in the data set and the range of x is $0 \le x \le 1$. Functions ϕ and W are the scaling and wavelet basis functions from which the function $f(x)$ is reconstructed. The index i can be uniquely expressed as $i = 2^j + k$, where j and k specify the resolution and the position of the wavelet. For instance, if $i = 18$ then $j = 4$ and $k = 2$ showing that a_{18} is the coefficient of the third of 16 wavelets at the $j = 4$ level whose widths are $1/2^4 = 1/16$ on the $x-$axis. A data set encoded in the time domain using N {*value, time*} pairs is thus transformed into a wavelet set encoded by N {*a-coefficient, index*} pairs.

3.1. Wavelet analysis: Time2Wave tools

Wavelet results for the higher resolution parts of the wavelet displays of industrial data set are presented in Figure 3. It shows the various frequencies present in the signals as time passes. The horizontal axis shows the position of the wavelet and the vertical axis is the resolution. High frequency features with a short time scale are at the top of the display and low frequency features at the bottom. The color coding indicates the intensity measured by the values of the *a*-coefficients. White or paler colors indicate higher intensity A Gabor wavelet was selected for the analysis.

Figure 4 shows the full wavelet analysis for tag 8 at all the resolution ranges including the low frequencies. It can be seen that parts of the wavelet display in the lower left and right corners are blank. The reason for this is that a wavelet analysis provides poorer time localization at lower resolution. Thus no analysis of the signal in the frequency band at 220 samples per cycle is possible until sufficient data have been sampled, which happens about one quarter of the way though the data seta about sample 900. It requires a window containing several cycles of the period 220 oscillation to make an analysis, therefore the first wavelet coefficient reported has several cycles to the left.

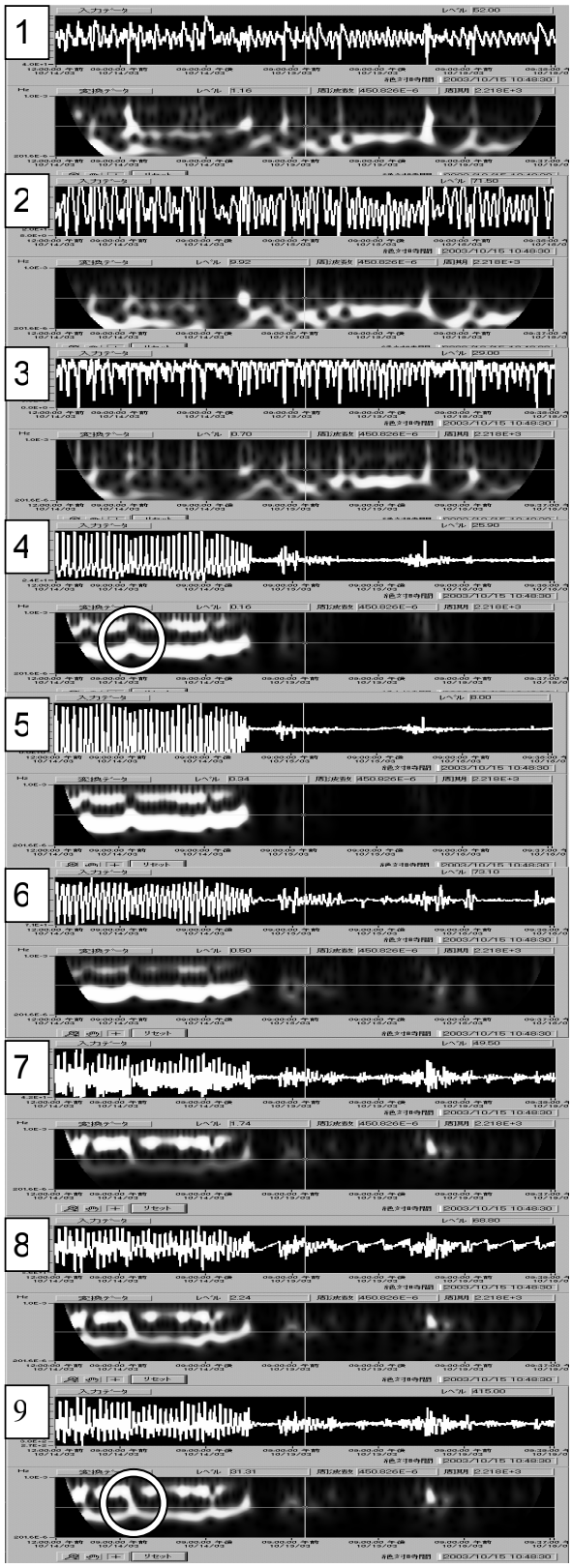

Figure 3. Wavelet analysis of measured time trends. The white circles are discussed in section 3.2.

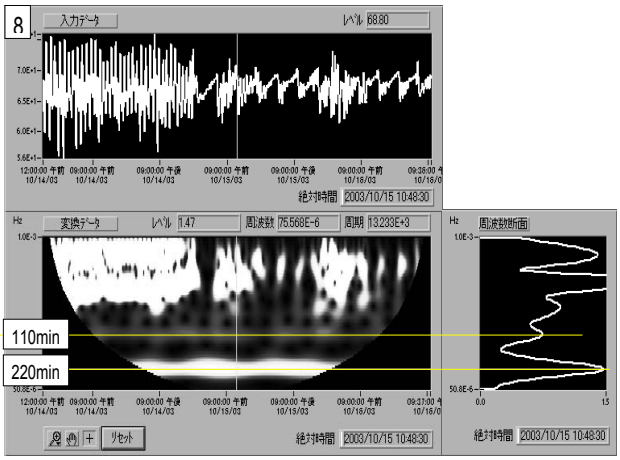

Figure 4. Wavelet analysis of Tag 8 showing a low frequency oscillation with a period of 220 min

The similarity of two wavelet patterns can be determined by a correlation calculation. Given two wavelet analysis such as those in Figure 3 the correlation coefficient is:

$$R = \frac{\sum (a_i - \bar{a})(b_i - \bar{b})}{\sum (a_i - \bar{a})^2 \sum (b_i - \bar{b})^2}$$

where a_i and b_i are the wavelet coefficients, $\bar{a}$ and $\bar{b}$ are their mean values and the index i ranges from 0 to $N-1$.

The *Time2Wave* tools also permit specific parts of the wavelet transforms to be compared. For instance, Figure 5 shows the comparison of the high frequency features for a target area in the time-frequency domain. The comparison is made at the same times and the same frequencies in the wavelet plots of the other tags. If $R = 1$ it means that the regions being compared have entire conformity with 100%.

3.2 Frequency and harmonics analysis

A frequency analysis is given by the power spectrum which is derived from the squares of the magnitudes of the discrete Fourier transform (DFT). Examples are shown in Figure 4. The horizontal axis is a normalized frequency axis expressed as a fraction of the sampling frequency. For instance, a spectral peak at 0.05 on the frequency axis corresponds to an oscillation having a frequency of $0.05 \times f_S$ where f_S is the sampling frequency. Such a peak corresponds with an oscillating time trend with a period of $1/0.05$ or 20 samples per cycle.

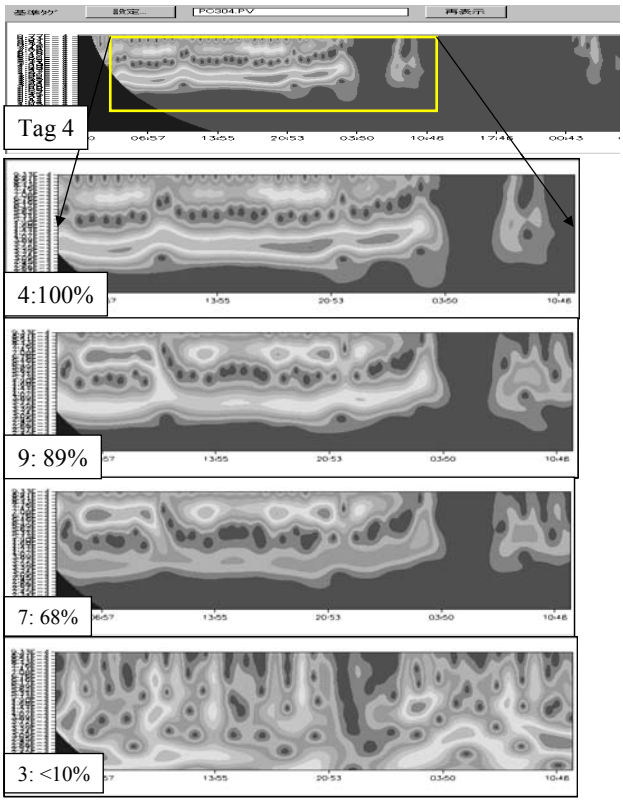

Figure 5. Comparison of high frequency features

In a set of time trends such as those shown in Figure 2 where the nature of the signal changes over time the Fourier transform has to be used on subsets of the data in order to observe the time-varying frequency content. In Figure 6 the middle panel shows the spectra for samples 1 to 1500, the right hand panel is the spectra for samples 2500 to 4000 and the left hand panel gives the spectra for the whole data set. The left hand panel shows all the frequencies present even though they are not all present simultaneously. The effect has a musical analogy, the spectrum cannot distinguish between a chord where all the notes are played simultaneously and a broken chord in which the notes are played one after the other. The wavelet transform, by contrast, can tell the difference because it determines when in time the different notes are being played. An example of the enhanced sensitivity of the wavelet transform to transient features is highlighted by white circles in Tags 4 and 8 in Figure 3. The bands with high intensity corresponding oscillations are disrupted for a short period. A very close inspection of the time trends in Figure 2 shows that the oscillation is a bit different between samples 600 to about 680 but it is likely that this transient feature would go unremarked if it were not for its strong visual signature in the wavelet transform. An inspection of the spectra in the middle panel of Figure 6 reveals nothing about the event because the spectra give no time-localization. It is not known,

however, what the disturbance was that upset the plant during this episode.

3.3 Oscillation analysis

The dominant oscillations present in the whole or a sub-set of the data may be determined visually by taking a slice through the wavelet transform parallel to the vertical resolution axis at a selected time instant, as shown in Figure 4. Alternatively, the automated method for detection of multiple plant-wide oscillations presented in [19]. may be applied, which determines the intervals between and the regularity of the zero-crossings of the autocovariance functions.

3.4 Diagnosis of non-linearity

A linear time series [20] has a dynamic model such as the Box Jenkins model with constant coefficients driven by Gaussian white noise. By contrast, the non-linear time series of interest in this work have a non-linear feedback function. An example of a non-linear feedback function is the on-off control of a directly-injected steam heated tank in which the steam valve switches on when the temperature drops to a low limit and switches off again when the temperature reaches a high limit. The non-linear characteristic in that case is a relay with deadband. The temperature is not steady in such a system and it cycles in periodic pattern. Another control loop non-linearity relevant to the work of this article is saturation of a manipulated variable. If an actuator hits a constraint then the discontinuity in its movement initiates a transient response which can lead to the actuator becoming saturated again. Such a repeating pattern is also a limit cycle.

A non-linearity test [21] has been adapted for the detection of limit cycle oscillations and guidelines for its application to process data have been devised. The question is whether a particular time series could plausibly be the output of a linear system driven by Gaussian white noise. The test is based on the predictability of the time series and return a non-linearity statistic N_S such that $N_S > 1$ indicates that the time series originated from a non-linear process. The development of the test for use with process data was described in [4] and a detailed investigation of its properties has been given in [22].

The underpinning idea in root cause diagnosis is that the non-linearity is greatest at the source of the problem. By source is meant a measurement associated with the single-input-single-output controller that has been caused to oscillate by a non-linearity in the loop. If plant-wide oscillation is due to limit cycling a candidate for the root cause is the time series with the maximum non-linearity.

3.5 A test for saturation

The range of values taken by the a DCS controller output signals is generally 0 to 100. Saturation is easily recognized visually because the time trend becomes flat and constrained either at a value of 0 or at a value of 100.

The proposed saturation test evaluates the statistical distribution of samples in short sequence of the time trend and tests whether the sequence matches tests sequences of the same length that are all 0 or all 100. The benefit of the statistical approach is that it can be applied to data having any arbitrary statistical distribution and requires little tuning.

The method used the *D*-statistic in the Kolmogorov-Smirnov two sample test. Given measurements y_i in a sequence the cumulative sample frequency function

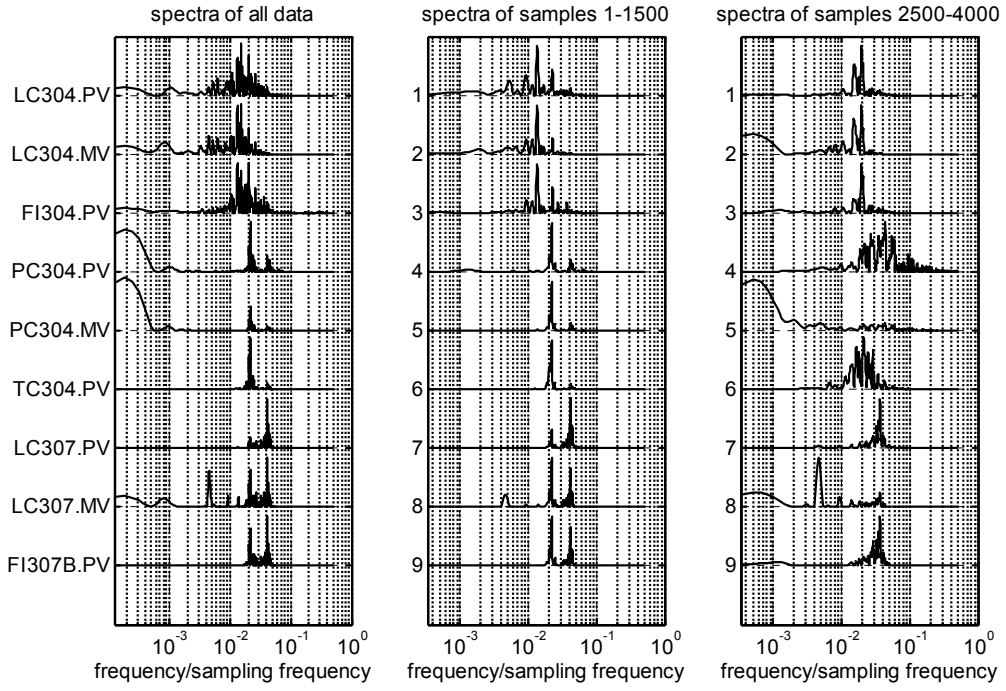

Figure 5. Spectra from the data set and sub-sets

$F(y_i \le y)$ is the fraction of the measurements y_i less than or equal to y. The Kolmogorov-Smirnov two-sample statistic for sequences S_1 and S_2 with cumulative sample frequency functions $F_1(y_i \le y)$ and $F_2(y_i \le y)$ is:

$$D = \max\left(\left|F_1(y_i \le y) - F_2(y_i \le y)\right|\right)$$

The sampling distribution of D can be found from published tables in the case of small samples or from an analytical approximation in the case of larger samples. The null hypothesis is that the observed value of D arose by chance when two sequences S_1 and S_2 were sampled from the same distribution. A large observed value of D corresponds with a small probability, and would lead to rejection of the null hypothesis that the sequences S_1 and S_2 were from matching distributions.

For instance, in tag 5 sample number 123 and the four previous values formed the sequence $\{6.9, 5.2, 3.4, 1.8, 0.1\}$ on a measurement scale having the range 0 to 100. The observed probability distribution is as shown in the first column of Table 1.

This distribution is to be tested against the distribution expected for a saturated output, i.e. the sequence $\{0, 0, 0, 0, 0\}$ whose cumulative distribution is shown in the right hand side of Table 1. The maximum difference is $D = 0.8$ in the $F(y_i \le 1)$ channel.

The Kolmogorov-Smirnov test indicates the probability is only 0.3 that sequences $\{6.9, 5.2, 3.4, 1.8, 0.1\}$ and $\{0, 0, 0, 0, 0\}$ were sampled from the same underlying distribution so it is concluded that $\{6.9, 5.2, 3.4, 1.8, 0.1\}$ does not represent saturated operation. On the other hand, the sequence of five values ending at sample 126 was $\{1.8, 0.1, 0, 0, 0\}$. Here the maximum difference in the cumulative distribution is 0.2 and the Kolmogorov-Smirnov test supports the null hypothesis that the sequence $\{1.8, 0.1, 0, 0, 0\}$ matches $\{0, 0, 0, 0, 0\}$ and therefore represents saturated operation.

Figure 7 shows episodes of saturated operation detected in the three MV tags by the procedure. The upper figure shows a close-up view and the lower figure shows the whole data set. It shows that Tag 5 (PC304.MV) ceased becoming saturated after the controller was retuned just after sample 1600 but that retuning of PC304 did not cure the periodic saturation in LC304..MV.

S_1={6.9, 5.2, 3.4, 1.8, 0.1}		S_2={0, 0, 0, 0, 0}	
$F_1(y_i \le 1)$	0.2	$F_2(y_i \le 1)$	1.0
$F_1(y_i \le 2)$	0.4	$F_2(y_i \le 2)$	1.0
$F_1(y_i \le 3)$	0.4	$F_2(y_i \le 3)$	1.0
$F_1(y_i \le 4)$	0.6	$F_2(y_i \le 4)$	1.0
$F_1(y_i \le 5)$	0.6	$F_2(y_i \le 5)$	1.0
$F_1(y_i \le 6)$	0.8	$F_2(y_i \le 6)$	1.0
$F_1(y_i \le 7)$	1.0	$F_2(y_i \le 7)$	1.0
$F_1(y_i \le 8)$	1.0	$F_2(y_i \le 8)$	1.0
…	…	…	…
$F_1(y_i \le 100)$	1.0	$F_2(y_i \le 100)$	1.0

Table 1: Worked example of the saturation test

4. Case study

4.1 Unit-wide oscillation

The industrial case study is courtesy of the Omuta works of Mitsui Chemicals. The plant schematic is in Figure 1 and data trends from the plant were presented in Figure 2. The sampling interval was 1 minute. Figures 3 and 4 showed the wavelet analysis and Figure 6 showed the spectra over different time ranges. The relationship between tag names and number is given in Table 2 because there is not enough room on some of the graphs to show the full tag name. A tag labeled as PV is a reading of a controlled variable (e.g. PC304.PV) or of an indicator (e.g. FI304.PV). The MV label means the measurement is a controller output.

Tag name	Tag No	Tag name	Tag No
LC304.PV	1	TC304.PV	6
LC304.MV	2	LC307.PV	7
FI304.PV	3	LC307.MV	8
PC304.PV	4	FI307B.PV	9
PC304.MV	5		

Table 2. Tag names and tag numbers

The dominant oscillations present determined using the zero crossings of autocovariance functions [19] are shown in Table 3. The table is divided into the period prior to retuning of PC304 and after.

samples 1-1500		samples 2000-4000	
Tag name	period/ min	Tag name	period/ min
LC304.PV	-	LC304.PV	51
LC304.MV	73	LC304.MV	51
FI304.PV	74	FI304.PV	51
PC304.PV	46	PC304.PV	-
PC304.MV	46	PC304.MV	-
TC304.PV	47	TC304.PV	35
LC307.PV	24	LC307.PV	29
LC307.MV	46, 24	LC307.MV	220
FI307B.PV	46, 24	FI307B.PV	29

Table 3: Dominant oscillations before and after retuning

Tag name	before retuning	after retuning
LC304.PV	1.6	2.1
LC304.MV	1.8	2.0
FI304.PV	2.0	1.9
PC304.PV	**2.5**	-
PC304.MV	**2.4**	-
TC304.PV	1.5	-
LC307.PV	1.3	-
LC307.MV	1.0	-
FI307B.PV	1.7	-

Table 4. Non-linearity assessment before and after retuning of PC304.

4.2 Oscillations before retuning

The oscillation that can be seen up to sample 1500 in Figure 2 had been persisting for some time prior to the study. By prior application of the wavelet transforms and from their knowledge and understanding of the process the Mitsui authors had already decided to retune the pressure control loop. The data set in Figure 2 documented the event by recording data from the day before the retuning, the retuning itself and about 40 hours of running after the retuning.

Visual inspection of time trends and wavelet patterns in Figures 2 and 3 show that the plant has a distinct oscillation up to samp1e 1500. The retuning occurred at about sample 1500 and the 46 minute oscillation then started to die away and it disappeared at about sample 1600. The analysis presented here shows that the retuning decision was justified and gives additional insights into the performance of the wavelet analysis tools.

Oscillation analysis before and after the retuning has been presented in Table 3. Non-linearity analyses were also carried out (Table 4) and saturation analysis is presented in Figure 7.

- The wavelet transforms (Figure 3) show Tags 4 to 11 have two bands of frequency content corresponding to oscillations with periods of about 46 min and 24 minutes. The spectra in the middle panel of Figure 6 show the same features with spectral peaks at 0.0217 and 0.0417 on the normalized frequency axis. The spectral peaks in Figure 5 reflect the intensities of the bands present in the wavelet transform. For instance, tag 7 has its strongest intensity in the upper of the two bands appearing on the left hand side of the wavelet transform (Fig 3) and in Figure 5 it is the tag with the strongest spectral peak at 0.0417.
- The wavelet transforms of Tags 1 to 3 also had well defined bands which were at a different position on the vertical resolution axis of the wavelet transform. The strongest oscillation present in Tags 1 to 3 had periods of 73 to 74 minutes and appears at 0.0135 on the frequency axis in the middle panel of Figure 5.
- Wavelet overlap calculations gave the results shown in Table 5 in which the wavelet transform of Tag 4, PC304.PV is compared to the wavelet transforms of other tags. The very high correlations with Tags 5, 6, 8 and 9 reflect the fact that these tags all share the oscillation with a period of 46 minutes. The dominant oscillation in Tag 7 is the one at 24 min and the correlation is lower. The correlation analysis shows that Tags 1-3 have little in common with Tag 4 and thus indicates that there are two separate disturbances present in the plant.

Tag name	Tag no	similarity
PC304.PV	4	100%
PC304.MV	5	98%
TC304.PV	6	93%
FI307B.PV	9	89%
LC307.MV	8	87%
LC307.PV	7	68%
LC304.PV	1	23%
LC304.MV	2	< 10%
FI304.PV	3	< 10%

Table 5. Overlap calculation for episode before retuning

- Non-linear time series analysis (Table 4) confirmed PC304 as the root cause of the unit–wide oscillation because the highest non-linearity was to be found in the pressure controller (PC304.PV and PC304.MV).
- The new saturation index confirmed the observation. Figure 7 shows that the loop was periodically becoming saturated. Therefore the cause of the problem is periodic saturation of the actuator.

Many previous examples of non-linearity in control loops have traced the root cause to a faulty valve or a

faulty sensor causing a self sustained limit cycle oscillation in a control loop [e.g. 23]

The example in this paper thus makes a new contribution to diagnosis of the root cause of a plant-wide oscillation because it shows an example in which non-linearity was detected even though all elements of the control loop were in a healthy state. Even a healthy valve cannot open beyond 100% or close beyond 0%, however, and some controller settings can cause such a saturation constraint to become active. The limit cycle arises because hitting the constraint sets in motion a transient response that later takes the control loop back into saturation. The new saturation index has the capacity diagnose such a problem.

4.3 After retuning of PC304

Key observations of the situation in the plant after sample 1600 are:

- Immediately after retuning the 46 minute oscillations in Tags 4, 5 and 6 (PC304.PV and PC304.MV and TC304PV) vanished simultaneously, but the oscillation of Tags 1 to 3 (LC304 and FI304.PV continued independently, although with a different oscillation period (76 minutes changed to 51 minutes).
- In all other tags the bight band corresponding to the oscillation at 46 minute oscillation disappeared when the PC304 controller was retuned. No non-linearity was detected in Tags 4-9 after the controller was retuned. and there was no further saturation in PC304.MV.
- Non-linearity was still present in tags 1 to 3. Tag 2, the manipulated variable for LC304 continued to have episodes of saturation. The fault in LC304 was not improved by the retuning of PC304. This finding shows that there is a second controller saturation problem present in the plant which is currently under investigation.
- After the retuning of PC304 an oscillation periodically burst into life in Tags 6-9. It is indicated in the wavelet transforms as bright localized spots. Its period was 29 minutes and therefore is different both from the 24 minute and 46 minute oscillation present in those tags before retuning. Further study is needed to determine the cause of the oscillation and to establish its relationship, if any, with the earlier oscillation.
- New behavior also became evident in LC307.MV after retuning. It is shown in Figure 2, where a continual ramping up and resetting sawtooth pattern can be observed with a repeat period of 220 samples per cycle. Figure 4 shows a more extended wavelet analysis of LC307.MV. The oscillation at 220 samples per cycle is a bright band across the lower part of the wavelet chart.

The time-localization properties of the wavelet transform are of great value in the analysis of this signal. An important finding from Figure 4 is that the 220 minute oscillation did not start at sample 1600 when the PC304 controller was retuned, rather it was present throughout. The origin of this slow oscillation in LC307.MV is currently under investigation by the Mitsui co-authors.

5. Conclusions

The paper has presented wavelet analysis tools designed for the purpose of detection of plant-wide disturbances and diagnosis of their root cause. The *Time2Wave* software allows visual inspection of the time-varying frequency content and has a plant-wide focus. For instance, it provides an automated and quantitative measure of the similarity between the wavelet transforms of any two selected measurements.

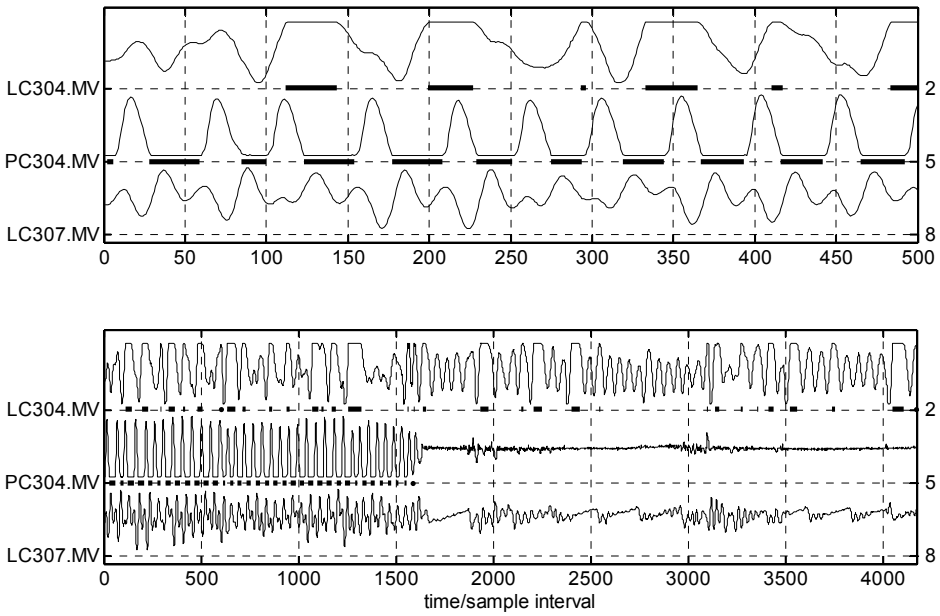

Figure 7. Saturation analysis. the heavy black lines below the time trends show episodes where a manipulated variable became saturated at 0% or 100%. Upper panel: close-up view of samples 1 to 500, lower panel: the whole of the data.

Insights from inspection of the wavelet transform led to a decision to retune the pressure controller PC304. The retuning activity was supported by non-linearity, oscillation and a new saturation detection analysis which were conducted before and after the retuning. Before re-tuning, PC304 was highlighted as the root cause of the 46 minute oscillation because the controller output PC304.MV was periodically becoming saturated and the PC304 control loop had significant non-linearity. After re-tuning there was no non-linearity and no saturation. This result has considerable implications because it shows that a limit cycle oscillation can take place in a control loop with no faulty components if the tuning is such that the controller output saturates at 0% or 100%.

There was a separate fault in LC304 and FI304 which did not go away when PC304 was re-tuned (the oscillation period changed, however). The time-localization properties of the wavelet transform were of benefit is establishing this finding because they showed visually that the re-tuning of PC304 had not had any significant impact. The controller output LC304.MV was periodically saturated throughout the case study and non-linearity was high in all of LC304.PV, LC304.MV and FI304.PV throughout, suggesting the need for retuning of LC304 to prevent the saturated condition from arising.

6. Acknowledgements

The authors thank Mr. Takashi Shigemasa, manager of Toshiba IT and Control System Corporation, for his valuable suggestion and Intelligent Manufacturing System (IMS) program for financial support during the study .Nina Thornhill gratefully acknowledges the financial support of the Royal Society (Study Visit to Japan Award).

7. References

[1] Shunta, J.P., 1995, *Achieving world class manufacturing through process control*, Prentice-Hall, NJ

[2] Qin, S.J. (1998). Control performance monitoring - a review and assessment. *Computers & Chemical Engineering*, 23, 173-186.

[3] Paulonis, M.A.,and Cox, J.W., 2003, A practical approach for large-scale controller performance assessment, diagnosis, and improvement. *Journal of Process Control*, 13, 155-168

[4] Thornhill, N.F., Cox, J.W., and Paulonis, M., 2003, Diagnosis of plant-wide oscillation through data-driven analysis and process understanding, *Control Engineering Practice*, 11, 1481-1490.

[5] Horch, A., 1999, A simple method for detection of stiction in control valves, *Control Engineering Practice*, 7, 1221-1231.

[6] McMillan, G.K. (1995). Improve control valve response. *Chem. Eng. Prog. (June)*, 77-84.

[7] Venkatasubramanian, V., Rengaswamy, R., Kavuri, S.N., and Yin, K., 2003, A review of process fault detection and diagnosis Part III: Process history based methods, *Computers & Chemical Engineering*, 27, 327-346.

[8] Kang, C.W., and Golay, M.W., 2000, Incorporation of modern on-line spectral condition monitoring for operational availability improvement of reactor coolant pumps, *Proceedings of the Institution of Mechanical Engineers Part E-Journal of Process Mechanical Engineering*, 214, 123-130

[9] Ansari, S.A., and Baig, R., 1998, A PC-based vibration analyzer for condition monitoring of process machinery, *IEEE Transactions on Instrumentation and Measurement*, 47, 378-383.

[10] Daubechies,I., Ten lectures on wavelets, *CBMS regional Conference Series in Applied Mathematics*, Philadelphia, PA., 1992.

[11] Mallat,S.G., A theory for multiresolution signal decomposition: the wavelet representation, *IEEE Trans Pattern. Anal. Mach. Intell,* 11, 764-693, 1989.

[12] Strang, G. and Nguyen, T., *Wavelets and filter banks*, Wellesley-Cambridge Press, Wellesley MA, USA, 1996.

[13] Sakakibara, S., 1995, *Beginner's Guide for Wavelet,* Publishing Bureau, Tokyo Denki University.

[14] Bakshi, B.R., and Stephanopoulos, G., 1993, Wave-net - a multiresolution, hierarchical neural network with localized learning, *AIChE Journal*, 39, 57-81.

[15] Stephanopoulos, G., Dyer, M., and Karsligil, O., 1997, Multi-scale modeling, estimation and control of processing systems, *Computers & Chemical Engineering* 21: S797-S803, 1997

[16] Peng, Z.K., and Chu, F.L., 2004, Application of the wavelet transform in machine condition monitoring and fault diagnostics: a review with bibliography, *Mechanical Systems and Signal Processing*, 18, 199-221.

[17] Misra, M., Yue, H.H., Qin, S.J., and Ling, C., 2002, Multivariate process monitoring and fault diagnosis by multi-scale PCA, *Computers & Chemical Engineering*, 26, 1281-1293.

[18] Matsuo,T. and Sasaoka, H., Application of Wavelet analysis to chemical process diagnosis, *KES'2002*, Crema, Italy(2002) 843-847

[19] Thornhill, N.F., Huang, B., and Zhang, H., 2003, Detection of multiple oscillations in control loops, *Journal of Process Control,* 13, 91-100

[20] Ljung, L., 1999, *System Identificatioin for the User*. Prentice Hall, New Jersey, USA.

[21] Kantz, H. and T. Schreiber (1997). *Nonlinear Time Series Analysis*. Cambridge University Press, Cambridge, UK.

[22] Thornhill, N.F., 2004, Finding the source of nonlinearity in a process with plant-wide oscillation, *submitted to IEEE Transactions on Control System Technology*

[23] Ruel, M., and Gerry, J., 1998, Quebec quandary solved by Fourier transform, *Intech (Aug)*, 53-55.